Universiteit
Leiden
The Netherlands

On shape and elasticity: bio-sheets, curved crystals, and odd droplets

Garcia Aguilar, I.R.

Citation
Garcia Aguilar, I. R. (2022, September 13). *On shape and elasticity: bio-sheets, curved crystals, and odd droplets*. *Casimir PhD Series*. Retrieved from https://hdl.handle.net/1887/3458390

Version:	Publisher's Version
License:	Licence agreement concerning inclusion of doctoral thesis in the Institutional Repository of the University of Leiden
Downloaded from:	https://hdl.handle.net/1887/3458390

Note: To cite this publication please use the final published version (if applicable).

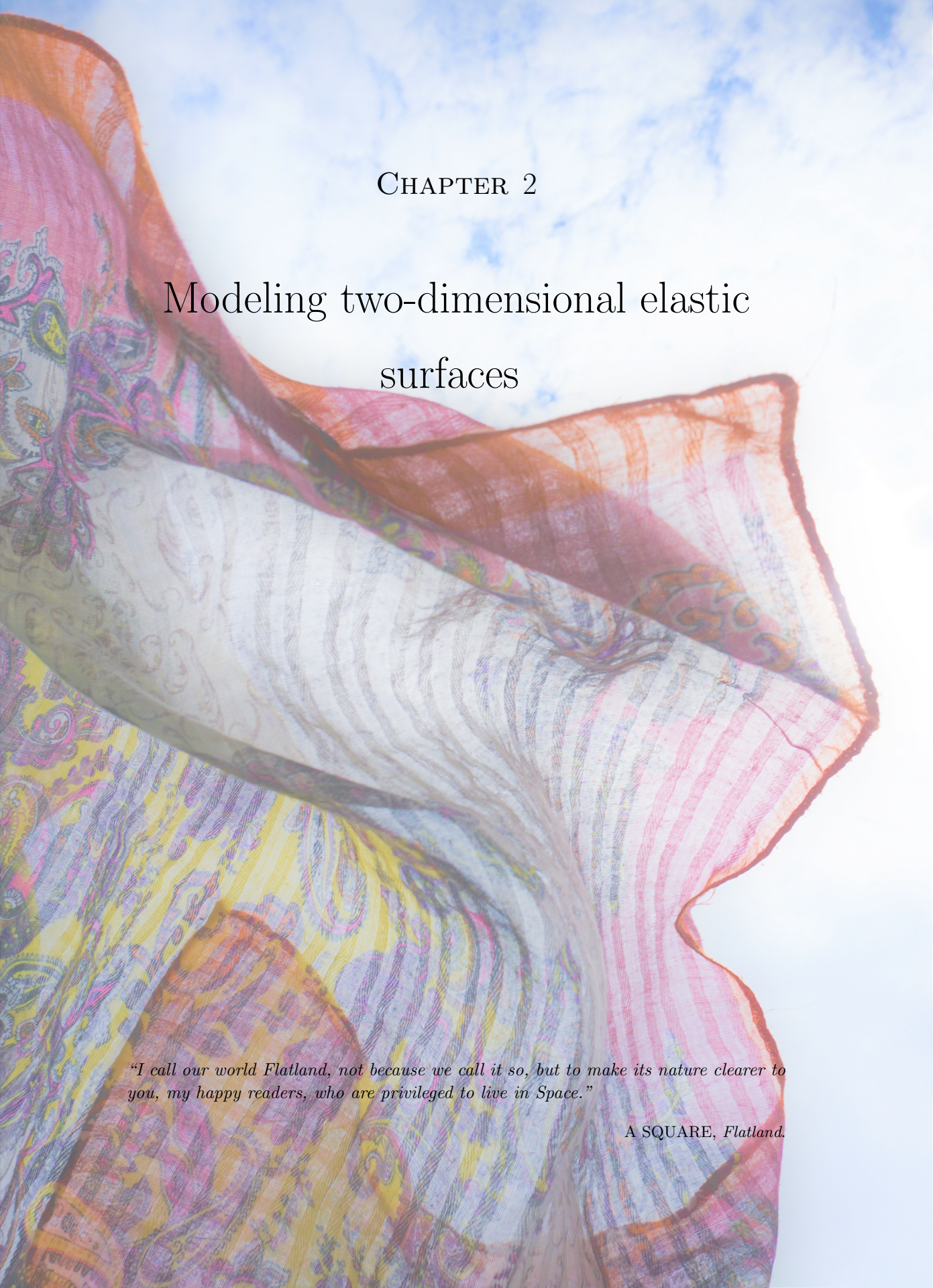

Chapter 2

Modeling two-dimensional elastic surfaces

"I call our world Flatland, not because we call it so, but to make its nature clearer to you, my happy readers, who are privileged to live in Space."

A SQUARE, *Flatland.*

Monolayered curved crystals, the interface of emulsion droplets and tubulin polymorphic assemblies can all be viewed as thin membranes of varying shape. We model these systems as effectively two-dimensional elastic surfaces but still embedded in our three-dimensional physical world, as they nonetheless bend, stretch and curve. In the Introduction, we outlined some basic concepts such as surface curvature and topology in a more intuitive way. To arrive to the mechanical description of surfaces we must however give formal definitions to these concepts in the language of differential geometry. Having covered the basics, we further explain how these definitions enter the models based on continuum linear elasticity theory of thin plates. We end the chapter explaining the practical implementation of surface elasticity on triangulated surfaces used for the three-dimensional computer modeling of thin membranes.

2.1 A story of 2D life in a 3D world Basics on curvature and geometry

The geometrical study of surfaces is set upon a base described in the language of differential geometry. In this section, we highlight those concepts which are necessary for the mechanical description of the thin elastic systems which we study in the remainder of the thesis. The basic concepts described here and further reading can be found in several other references, including Refs. [2, 18, 64, 65].

2.1.1 Measuring length

Consider a two-dimensional curved smooth[1] surface S of an arbitrary shape, which is embedded in our familiar three-dimensional space. The parametrization of the surface maps an appropriate two-coordinate system to the three-dimensional position vectors of all points on that surface, $\boldsymbol{r}(x^1, x^2)$. In general, we will distinguish three-dimensional vectors with bold letters, $\boldsymbol{r}$, while components of vectors and tensors defined on the two-dimensional surface carry index notation; for example, x^i for $(i = 1, 2)$. At any given point on S, we can define the tangent vectors

$$\boldsymbol{e}_i = \frac{\partial \boldsymbol{r}}{\partial x^i} \quad (i = 1, 2)\,. \tag{2.1}$$

In general, $\boldsymbol{e}_i$ are not unit vectors, nor are they necessarily orthogonal [2] . In fact, the *metric tensor* of the surface, whose covariant components are defined by the inner product of the tangent vectors,

$$g_{ij} = \boldsymbol{e}_i \cdot \boldsymbol{e}_j\,, \tag{2.2}$$

[1] In this thesis, we are exclusively concerned with "well-behaved" orientable surfaces where all the descriptions on this chapter are applicable and allowed [65].

[2] However, the parametrization $\boldsymbol{r}(x^1, x^2)$ only defines a smooth surface if the tangent vectors $\boldsymbol{e}_i$ are linearly independent [65].

encodes the correct description of distances on a particular surface. The contravariant components of the metric tensor, g^{ij}, are defined such that

$$g_{ij}g^{jk} = \delta_i^k = \begin{cases} 1 & \text{if } i = k \\ 0 & \text{if } i \neq k \end{cases} , \tag{2.3}$$

where δ_i^k is the Kronecker delta, or the components of the unit matrix. Consider some vector on the tangent plane of S, expressed in the basis of the tangent vectors $\boldsymbol{a} = a^k \boldsymbol{e}_k$ [3] . Given the definition above, Eq. (2.3), the metric tensor can be used to lower/raise indices, i.e., $a^i = g^{ij}a_j$ and $a_i = g_{ij}a^j$. So, in general, the scalar product of two vectors tangent to the surface can be written as $\boldsymbol{a} \cdot \boldsymbol{b} = g_{ij}a^i b^j$.

The name choice for the metric tensor becomes more evident when calculating for example the line element or the area element for a given coordinate system. The *first fundamental form* on S is given by

$$ds^2 = g_{ij}dx^i dx^j , \tag{2.4}$$

where $ds = \sqrt{ds^2}$ is the line element on the surface or the distance between a point P and a point Q on the surface which are infinitesimally close by. Taking the determinant of the metric tensor $g = |g_{ij}|$, the area element on S can be expressed as

$$dA = |\boldsymbol{e}_1 dx^1 \times \boldsymbol{e}_2 dx^2| = \sqrt{g}\, dx^1 dx^2 . \tag{2.5}$$

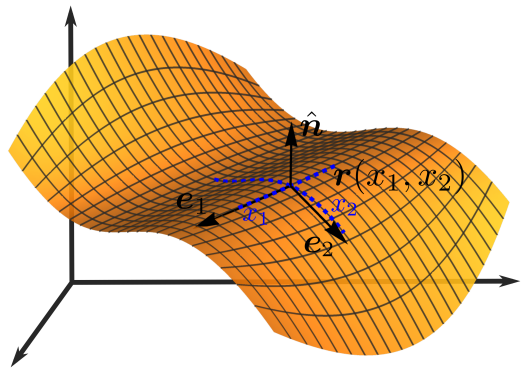

Figure 2.1: Local frame on a two-dimensional surface S embedded in three-dimensional space. At any point P on the surface, with position vector $\boldsymbol{r}(x^1, x^2)$, we can calculate two tangent vectors $\boldsymbol{e}_i$, and a normal unit vector $\hat{\boldsymbol{n}}$. For a given coordinate system x^i, we can extract the local geometric properties of interest from the metric tensor g_{ij} and the extrinsic curvature tensor b_{ij} of the surface.

2.1.2 The covariant derivative

Say that we are interested in the directional derivative of the vector field $\boldsymbol{a} = a^k \boldsymbol{e}_k$ along the surface coordinate x^i. Unlike the friendly Cartesian system of flat space, the basis $\boldsymbol{e}_k$ itself also depends on the local coordinates. The *covariant derivative*

[3] Here and for the rest of the chapter, we follow the commonly used Einstein convention for summation: having the same dummy index twice in a given term, once as a subscript (covariant) and once as a superscript (contravariant), implies summing over this index, i.e. $a^i b_i = \sum_i a^i b_i$.

∇_i, is the operator acting as the correct generalization of directional derivation on a curved space defined as

$$\nabla_i a^k = \frac{\partial a^k}{\partial x^i} + a^j \Gamma^k_{ij} \,, \tag{2.6a}$$

$$\nabla_i a_k = \frac{\partial a_k}{\partial x^i} - a_j \Gamma^j_{ik} \,, \tag{2.6b}$$

where Γ^k_{ij} is called the *Christoffel symbol*, given by $\Gamma^k_{ij} = g^{kl}\Gamma_{ijl}$, and

$$\Gamma_{ijl} = \frac{\partial \boldsymbol{e}_i}{\partial x^j} \cdot \boldsymbol{e}_l \,. \tag{2.7}$$

This expression emphasizes how the Christoffel symbols contain the variation of the tangent basis vectors as one moves along the surface. The covariant derivative ensures that the directional derivation of a field on the surface does not depend on the coordinate system used. In other words, the derivative in Eq. (2.6) do transform as a tensor under a change of coordinates. It is therefore the relevant operator for physics on two-dimensional curved surfaces for which the metric is different than the unit matrix[4].

2.1.3 Measuring curvature

To quantify the curvature at some point P, we need to look at how the two-dimensional surface is embedded in three-dimensional space. Consider the normal vector to the surface,

$$\hat{\boldsymbol{n}} = \frac{\boldsymbol{e}_1 \times \boldsymbol{e}_2}{|\boldsymbol{e}_1 \times \boldsymbol{e}_2|} \,. \tag{2.8}$$

Another important tensor for the geometrical description of a two-dimensional surface is that defined in the *second fundamental form* on S,

$$2h = b_{ij} dx^i dx^j \,, \tag{2.9}$$

where b_{ij} are the covariant components of the *extrinsic curvature tensor*, defined by

$$b_{ij} = \boldsymbol{e}_i \cdot \frac{\partial \hat{\boldsymbol{n}}}{\partial x_j} \,. \tag{2.10}$$

The invariant h can be interpreted as the distance to the tangent plane at a point P of a point Q on the surface which is infinitely close by [2] or, in other words, how much the surface is pulled along the normal direction. While the metric tensor describes distances on the surface itself, the extrinsic curvature tensor encodes how the surface is embedded in three-dimensional space. Since $\hat{\boldsymbol{n}}$ is a unit vector, b_{ij} keeps track of how the normal vector changes orientation as one moves tangentially to the surface.

Standing on P, there are an infinite number of tangent directions to the surface. Take one of these, described by the unit vector $\boldsymbol{t} = t^i \boldsymbol{e}_i$. The *normal curvature* of the

[4]For example, the additional term in the covariant derivative ensures that when transporting along a surface a vector that lives in the tangent plane, the vector remains tangent to the surface.

surface for that direction, given by the inverse radius of the osculating circle along the surface projection on the plane $\boldsymbol{t}$ and $\hat{\boldsymbol{n}}$ is given by

$$\kappa_n = b_{ij} t^i t^j \,. \tag{2.11}$$

We note that the positive sign in Eq. (2.10) is a convention that defines the sign of the curvature value. Under this convention, a sphere –which has constant normal curvature everywhere– has positive curvature (see Fig. 2.2). The two directions for which the normal curvature of the surface is extremal are called the principal directions and they correspond to the eigenvectors of the extrinsic curvature tensor [64]. Since b_{ij} is symmetric, the principal directions are orthogonal to each other. The eigenvalues are called the principal curvatures of the surface, κ_1 and κ_2.

Given the principal curvatures, we further define three scalars as measures of the curvature of surface S:

$$H = \frac{\kappa_1 + \kappa_2}{2} \qquad \textit{Mean curvature}, \tag{2.12a}$$

$$\Omega = \frac{|\kappa_1 - \kappa_2|}{2} \qquad \textit{Warp or Deviatoric curvature}, \tag{2.12b}$$

$$K = \kappa_1 \kappa_2 \qquad \textit{Gaussian curvature}. \tag{2.12c}$$

These three quantities describe the local curvature at P and are invariant under reparametrizations of the surface.

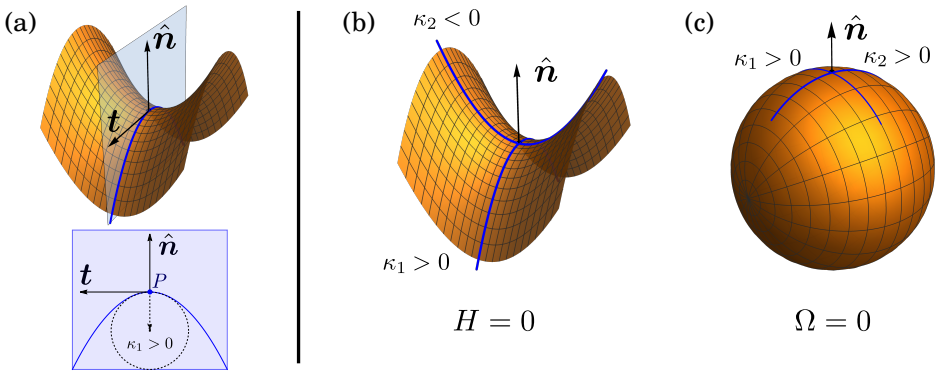

Figure 2.2: Local surface curvatures at point P. (a) The normal curvature for a given direction $\boldsymbol{t}$, Eq. (2.11), is determined by the projection of the surface onto the plane described by $\boldsymbol{t}$ and the normal vector $\hat{\boldsymbol{n}}$, colored in blue. The curvature κ is the inverse radius of the osculating circle at P, and it is defined positive for a line curving away from the surface normal. (b) The projected maximal and minimal values are the principal curvatures of the surface κ_1 and κ_2. A symmetric saddle has principal curvatures of the equal magnitude but opposite sign, and therefore the surface at P has negative Gaussian curvature and no mean curvature. (c) A sphere instead, for which all surface curvatures are positive and have the same magnitude, has no deviatoric curvature and positive Gaussian curvature everywhere. The saddle and the sphere illustrate two independent modes of curvature: a pure elliptical one quantified by H, and a hyperbolic one Ω.

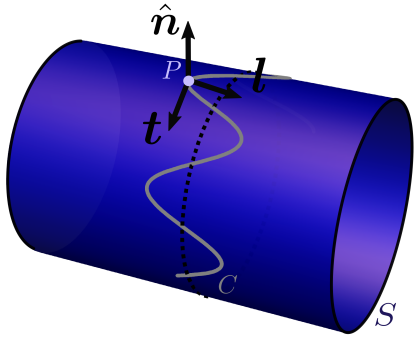

Figure 2.3: Curvature decomposition of a meandering curve C on surface S. As seen extrinsically, the white curve has two components to the line curvature $\boldsymbol{\kappa}$ at point P: a term along the surface $\kappa_{\boldsymbol{t}}\hat{\boldsymbol{n}}$ which is precisely the normal curvature of the surface itself; and a tangential term along $\boldsymbol{l}$ called the geodesic curvature κ_g. A plain open surface can also have some geodesic curvature at the boundary (imagine creating a new boundary by cutting the cylinder along the white line). However, the integral of the Gaussian curvature on S and the integral of the geodesic curvature along ∂S are topologically related through χ, as seen from Gauss-Bonnet theorem in Eq. (2.15).

Finally, we define the *geodesic curvature* of a curve on a surface S which, in this thesis, becomes relevant for surfaces with boundaries. Imagine some curve C drawn meandering on the surface S, such as the white curve in Fig. 2.3. The way this line curves in space is partially due to being forced to follow the natural bending of the surface, highlighted by the dash line, and partially because of the curvature of the line itself. The first contribution is precisely the normal curvature of the surface along the tangent to C, $\kappa_{\boldsymbol{t}}$ given in Eq. (2.11). The latter instead is the geodesic curvature and it is independent of surface curvature. In other words, if $\boldsymbol{t}$ is the tangent vector to the curve C at some point, the line curvature vector of C, $\boldsymbol{\kappa}$ is

$$\boldsymbol{\kappa} = \kappa_{\boldsymbol{t}}\hat{\boldsymbol{n}} + \kappa_g \boldsymbol{l}\,, \tag{2.13}$$

where $\boldsymbol{l} = \hat{\boldsymbol{n}} \times \boldsymbol{t}$. A curve which exactly follows the normal curvature of the surface is called a geodesic and it has $\kappa_g = 0$ [5]. In an open surface, the curvature at its boundary is quantified by its geodesic curvature. For example, the solid black boundary of the cylinder in Fig. 2.3 has $\kappa_g = 0$. Yet, cutting the cylinder along the white line results in a boundary with $\kappa_g \neq 0$.

2.1.4 Developable surfaces

As opposed to the extrinsic curvature, defined as $2H$, the Gaussian curvature is in fact an intrinsic property of the surface and does not depend on the specific embedding, even though K is also extracted from the extrinsic curvature tensor b_{ij}. This surprising result was derived by Gauss, which he called the *Theorema Egregium*, or remarkable theorem [6]. The Gaussian curvature instead is solely connected to the metric. So long as a surface is not stretched or compressed, one can bend it in different ways, thus locally changing the mean and deviatoric curvatures, H and Ω, but keeping K unchanged.

[5] The distance between two points on S is shortest along the surface geodesic.
[6] Also translated as "brilliant" or "outstanding" depending on the reference

To illustrate this, imagine bending some surface that does not really allow for stretching, such as a flat sheet of paper (see Fig. 2.4). Bending it into a cylinder of radius R will keep the area element (Eq. (2.5)) unchanged but it will clearly change the local curvature. However, while $H = \Omega = 1/(2R)$ everywhere, the cylinder has no Gaussian curvature, as the surface is essentially flat along one of the principal direction. In fact, this is true for any other continuous deformation which preserves the measure of distance on the surface, also called *isometric* deformations. We use the distinction here that *bending* relates to isometric deformations while *curving* changes the Gaussian curvature of the surface [7]. Formally, a smooth surface which has zero Gaussian curvature everywhere is called a *developable surface*.

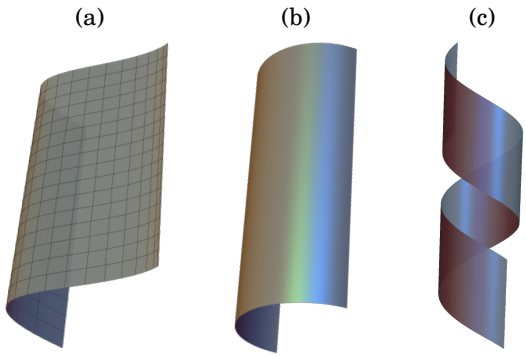

Figure 2.4: Developable surfaces. (a) Isometric, or distance-preserving, deformations bend a flat plane, similar to bending a rigid piece of paper. The surface remains developable, as $K = 0$ everywhere. Open sheets can bend into other developable geometries such as (b) cylinders and (c) helical ribbons.

2.1.5 Connecting geometry to topology

As first described by Leonhard Euler in 1758, for any convex polyhedron, the number of faces F, the number edges E and the number of vertices V are related through a single constant: $F - E + V = 2$ [66]. In fact, the Euler formula can be generalized for other surfaces when described through some polygonization, as

$$F - E + V = \chi \,, \tag{2.14}$$

where the particular constant χ, called *Euler characteristic*, is determined by the topology of the surface. Indeed, for any closed shape that can be continuously deformed into a sphere, such as a polyhedron, the Euler characteristic is $\chi = 2$ (see also Fig. 1.1).

We introduce here the Euler characteristic in order to highlight an exceptional connection between surface topology and the global nature of its intrinsic curvature.

[7] As explained further below, the latter also implies stretching.

The Gauss-Bonnet theorem in two dimensions for a surface S is expressed as:

$$\int_S K dA + \int_{\partial S} \kappa_g \, dl = 2\pi\chi \,, \tag{2.15}$$

relating the topological constant χ to the integral of the Gaussian curvature K over the surface and the integral of the geodesic curvature κ_g of the boundary of said surface.

Note that for surfaces without a boundary, such as those of spherical topology, the Gauss-Bonnet theorem states that for any continuous deformation, the integral of the Gaussian curvature remains a constant. In other words, if the surface is deformed locally increasing K somewhere, the deformation is accompanied by a decrease of the local curvature somewhere else [8]. In the case of surfaces with boundaries, such as a rectangular sheet, such K-increasing deformations can also be translated in changes of the geodesic curvature of its boundary.

The Gauss-Bonnet theorem, as expressed in Eq. (2.15), must be slightly modified when the boundary of S has sharp corners or points where the tangent vector varies discontinuously along the contour ∂S:

$$\int_S K dA + \int_{\partial S} \kappa_g \, dl + \sum_i^{\text{corners}} \alpha_i = 2\pi\chi \,, \tag{2.16}$$

where α_i is called the *jump angle* at a given corner. This is the angle difference between the tangent vectors at the corner. The integral of κ_g is then only along the continuous bits of the boundary.

2.2 Mechanical energy of an elastic thin sheet

In the absence of external forces, the mechanics of an elastic solid is governed by internal stresses sourced by deformations from a reference state. In general for three-dimensional solids, small strains in the material lead to small deformations. However, in the case of thin sheets, the material can have large bending deformations from small planar strains when deformed along the thin dimension. For effectively vanishing thickness, such as for the two-dimensional surfaces we study in the following chapters, the elastic energy can be expressed as the sum of two contributions: the stretching energy rising from tangential deformations, and the bending energy quantifying out-of-plane deformations along the surface normal:

$$E = E_{\text{bend}} + E_{\text{stretch}} \,. \tag{2.17}$$

In the rest of this section we expand on how we calculate these two terms for a curved elastic surface. We highlight an implicit interplay between stretching and curving of the surface which we further explore in Chapter 3. The explicit competition between the bending and stretching energy terms is relevant in Chapter 4 and Chapter 5.

[8] In a deformation of a sphere into a icosahedron, for example, the constant Gaussian curvature gets re-destributed into vertices with much larger K but flatter faces with vanishing K. This will be relevant in Chapter 3.

2.2.1 Bending energy

Helfrich energy

In 1973, Helfrich proposed an expression for the bending energy of a thin membrane as an expansion on the surface curvature scalars in Eq. (2.12), which also takes into account the spontaneous curvature [15]. The Helfrich bending energy is

$$E_{\text{bend}} = \int dA \left[2k \left(H - H_0 \right)^2 + \tilde{k} K \right] , \tag{2.18}$$

where H_0 is the mean spontaneous curvature[9], and the material moduli are often referred to as the *bending rigidity* k and the *saddle splay modulus* $\tilde{k}$. We take H_0 to be constant, as originally proposed, since this is expected in single component systems.

Helfrich formulated Eq. (2.18) in the context of lipid membranes where the bending energy is the only component in the elastic energy. This expression is often also found without the second term on the right hand side, especially in closed systems without boundaries. As we see from the Gauss-Bonnet theorem in Eq. (2.15), upon integration of the energy density over the surface, the Gaussian curvature integral results in a topological constant plus a boundary integral. The latter is zero for closed surfaces or simply a constant for open topologies whose boundaries remain fixed, and can therefore be neglected in these cases.

Fischer energy

In 1992, Fischer proposed a different expression for the bending energy [67], considering the fact that, following Eq. (2.12), the Gaussian curvature can be decomposed in terms of the (isotropic) mean curvature and the deviatoric curvature:

$$K = H^2 - \Omega^2 = \frac{\left(\kappa_1 + \kappa_2 \right)^2}{4} - \frac{\left(\kappa_1 - \kappa_2 \right)^2}{4} . \tag{2.19}$$

Based on this decomposition, Fischer suggests a more intuitive expression of bending energy using H and Ω as two independent curvature modes [67]:

$$E_{\text{bend}} = \int dA \left[k_H \left(H - H_0^{(F)} \right)^2 + k_\Omega \left(\Omega - \Omega_0 \right)^2 \right] , \tag{2.20}$$

where the material moduli k_H and k_Ω are the coupling energy constants respectively. The two modes are best illustrated by the spherical surface and the symmetric saddle in Fig. 2.2. At the saddle point in panel b, the two principal curvatures have the same absolute value but opposite sign because of their orientation with respect to the normal $\hat{\boldsymbol{n}}$, and thus the $H = 0$. Conversely, on top of the spherical cap in panel c, the principal curvatures have the same sign, so $\Omega = 0$. The actual curvature at a point of a generic surface is a superposition of these two independent modes, and

[9] To be more precise, Helfrich proposed his model considering the extrinsic curvature $2H$ and therefore using a spontaneous curvature $C_0 = 2H_0$

in a similar way, so is the spontaneous curvature in general. The energy Eq. (2.20) therefore contains not only the spontaneous mean curvature H_0 but also a spontaneous deviatoric curvature Ω_0.

From Eq. (2.19) we read that the deviatoric component is larger for a point with negative Gaussian curvature. Since $K = \kappa_1\kappa_2$, this translates into bending the surface in opposite directions along perpendicular orientations, generating a twist – or warp. In general, we refer to H_0 as the *spontaneous mean curvature* and to Ω_0 as the *spontaneous warp*. In the absence of spontaneous warp, just like assumed by Helfrich, both energy formulations are equivalent up to a combination of the material constants [68], for

$$k_H = k + \tilde{k}\,, \qquad k_\Omega = -\tilde{k}\,. \tag{2.21}$$

In Eq. (2.20), we make the distinction between the spontaneous mean curvature $H_0^{(F)}$ and that in the Helfrich model, Eq. (2.18), as these differ by a scaling factor

$$H_0^{(F)} = H_0 \frac{k}{k+\tilde{k}}\,, \tag{2.22}$$

when $\Omega_0 = 0$. Unless necessary due to context, we further drop the superscript for the spontaneous curvature in the Fischer formalism.

To Helfrich or to Fischer?

In chapter 4 we are concerned with the mechanics of the elastic interface of emulsion droplets. These are essentially surfaces of spherical topology for which, having no boundary, the integral of the Gaussian curvature over the whole surface simply integrates to 4π. We therefore use the Helfrich formalism for the bending energy in this chapter, considering only the first term in Eq. (2.18), related to the mean curvature. Moreover, the monolayer interfaces studied in this chapter are composed of surfactant molecules which are rotational symmetric along the surface normal. Because of similar to arguments used for lipid vesicles in Refs. [67, 68], in this system $\Omega_0 \approx 0$, and so both formalisms for the bending energy are equivalent.

In chapter 5 instead, we use the Fischer expression in order to account for observed mechanical anisotropy in tubulin assemblies. Insights from the study of microtubule dynamics suggest that the molecular architecture of tubulin can be tuned by assisting proteins or ions in cells which could give rise to saddle-like curvatures. Additionally, for open disk topologies the integral of the Gaussian curvature is no longer always a constant energy shift, as there are additional boundary terms.

2.2.2 Stretching energy

The stretching contribution in Eq. (2.17) comes from tangential deformations which cannot be relaxed and therefore have some energy cost. In continuum elasticity theory, the deviation of the surface from a reference state $\boldsymbol{r}(x^1, x^2)$ into a deformed state $\boldsymbol{r}'(x^1, x^2)$ is quantified by the *deformation vector field* $\boldsymbol{u} = \boldsymbol{r}' - \boldsymbol{r}$. Tangential deformations lead to changes in the distances between points on the surface, or as seen

from the fist fundamental form Eq. (2.4), changes in the metric tensor for a given coordinate system. The *strain tensor* contains the information of this change,

$$u_{ij} = \frac{1}{2}(g'_{ij} - g_{ij})\,, \tag{2.23}$$

where g_{ij} is given in Eq. (2.2), and g'_{ij} is the metric for the deformed state:

$$g'_{ij} = \frac{\partial \boldsymbol{r}'}{\partial x^i} \cdot \frac{\partial \boldsymbol{r}'}{\partial x^j}\,, \tag{2.24}$$

Expressing the deformation vector in the basis of the tangent vectors $\boldsymbol{u} = u^i \boldsymbol{e}_i$, the strain tensor is written in a way more familiar to the general theory of elasticity of solids [1],

$$u_{ij} = \nabla_j u_i + \nabla_i u_j + \nabla_i u^k \nabla_j u_k\,, \tag{2.25}$$

but in terms of the covariant derivative Eq. (2.6), appropriate for our curved surfaces.

The stretching energy is given by an expansion in the strain tensor [1],

$$E_{\text{stretch}} = \int dA \left(\frac{1}{2}\lambda {u_i^i}^2 + \mu u_{ij} u^{ij}\right)\,, \tag{2.26}$$

where λ and μ are the *Lamé coefficients* in two dimensions. These can be expressed in terms of the two-dimensional *Young's modulus* Y and the *Poisson ratio* ν,

$$\lambda = \frac{Y\nu}{1-\nu^2}\,, \tag{2.27a}$$

$$\mu = \frac{Y}{2(1+\nu)}\,. \tag{2.27b}$$

In linear elasticity theory, deformations are assumed to come from small strains, for which $u_{ij} \approx \nabla_j u_i + \nabla_i u_j$. The internal forces generated by the distortion are contained in the *stress tensor*, σ_{ij}, found from the minimization of Eq. (2.26) in the absence of body forces. We then write Hooke's law as

$$\sigma_{ij} = \frac{Y}{(1+\nu)} u_{ij} + \frac{Y\nu}{1-\nu^2}\; g_{ij} u_k^k\,. \tag{2.28}$$

From Hooke's law, a Poisson equation can be derived for the trace of the stress tensor, $\sigma = \sigma_i^i$ [69]. For an incompressible curved sheet, i.e. $\nu = 1$, the equation becomes

$$\nabla^2 \sigma = -Y\;\delta K\,, \tag{2.29}$$

where

$$\nabla^2 = g^{ij}\nabla_i \nabla_j \tag{2.30}$$

is the *Laplace-Beltrami operator*, the generalization of the Laplacian operator for curved manifolds. Analogously to the Gauss's law in electrostatics, here the variation of the Gaussian curvature acts as a source term to the surface stress, taking us back to the connection between the intrinsic curvature and the metric tensor. This variation can be due to curving of the surface itself, as we see for the open elastic sheets in

Chapter 5. The source term can also include additional in-plane deformations from the breaking of the orientational or the translational order in regular two-dimensional crystals. In this case, the presence of topological defects is expressed into the right-hand side of Eq. (2.29), as we elaborate further in Chapter 3 where we look at the connection between defect stretching and the intrinsic curvature for closed crystals. Finally, for incompressible surfaces, the stretching energy depends only on the two-dimensional Young modulus and is written in general as

$$E_{\text{stretch}} = \frac{1}{2} Y \int dA\, \hat{\sigma}^2 \,, \tag{2.31}$$

where we consider the dimensionless stress tensor $\hat{\sigma} = \frac{1}{Y}\sigma$.

2.3 Elasticity on a discretized surface

So far we have made an important assumption that the thin sheet systems which we are interested in, can be essentially modeled as two-dimensional elastic surfaces. Using concepts from differential geometry as a basis, we built up towards an expression of the mechanical energy suitable for curved thin sheets, with the surface parametrization $\boldsymbol{r}(x^1, x^2)$ as the starting point. The bad news is that for most geometries, calculating all geometric quantities that trickle down from this is either not an easy task or there is no parametrization at all to begin with (there is a reason why cows are modeled as spheres). The good news is that it is possible to calculate the geometric fields introduced in Section 2.1 on discretized versions of the elastic surface of interest, and in particular on triangulated meshes, such as that in Fig. 2.5a. Except on the rare occasion, in this thesis we work with triangulated versions of the various surface geometries.

2.3.1 Geometric fields on a triangulated surface

A triangulated mesh with N_v vertices is described by the position vectors of these vertices $\boldsymbol{r}_v$, and their connectivity, given by a list of index triplets defining the triangular faces making up the surface. For all surfaces, we keep the topology of the mesh fixed.

The geometric fields of interest, such as the local curvatures in Eq. (2.12), are numerically calculated at each vertex. Discrete methods for triangulated surfaces is a field of its own but we make use of the geometric differential operators presented in Ref. [70]. In this framework, the various geometric quantities at some vertex are approximated as spatial averages around it and restricted only to its immediate neighbors [10]. So, for a vertex i and its neighborhood (such as illustrated in Fig. 2.5b), these quantities are given as sums over the neighboring vertices. Since the mesh topology is fixed, we rewrite the expressions in Ref. [70] as sums over the neighboring triangles instead. In other words, we consider sums over the triangles t consisting of those triplets $t = \{i, j, k\}$ containing i. For the triangle-based calculation of the

[10] Also referred as the 1-ring neighborhood

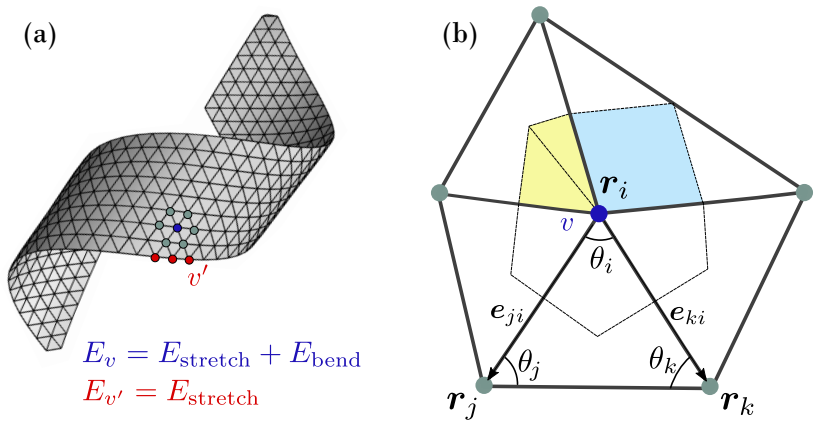

Figure 2.5: Surface discretization and relevant geometric quantities. In practice, we work with triangulated surfaces of the two-dimensional geometries that we study. a) A smooth helix is approximated by a mesh of $N_v = 369$ vertices. The number of vertices varies according to how computational demanding is the specific energy implementation. The geometric quantities are defined at each vertex i and calculated from spatial averages in the nearest neighborhood, such as the one illustrated in b). These averages can be rewritten as a sum on the neighboring triangles $t = \{i, j, k\}$, or those triplets containing vertex i, and the normal direction is encoded in the triplet permutation. Each vertex is assigned a portion of the area of the neighboring triangles within dashed lines, which is either the Voronoi region for non-obtuse triangles (yellow region), or a fixed fraction if the triangle is obtuse (blue region), as seen in Eq. (2.32).

different terms, it is useful to keep in mind the schematic in Fig. 2.5b. This shows the neighborhood of a vertex i, and the relevant quantities for a particular triangle t defined by i at position $\boldsymbol{r}_i$, and the neighboring vertices j and k at $\boldsymbol{r}_j$ and $\boldsymbol{r}_k$. In particular, all quantities can be described in terms of the edge vectors $\boldsymbol{e}_{ab} = \boldsymbol{r}_a - \boldsymbol{r}_a$, their magnitudes $r_{ab} = |\boldsymbol{e}_{ab}|$, and the internal angles of the triangle θ_i, θ_j and θ_k.

Vertex area

Each vertex i is assigned an area patch $A_i = \sum_t A_i^{(t)}$ in a way that all vertex patches in the mesh perfectly tile the whole surface. Commonly, the *Voronoi tessellation* is used to determine $A_i^{(t)}$, which consists of the region of points in triangle t which are closest to i as opposed to j or k. In Fig. 2.5b for example, the region colored in yellow is the Voronoi area of i for that specific triangle. The Voronoi area per triangle can be calculated from the cotangent weights used to approximate the discrete Laplace-Beltrami operator [70]. However, if the neighboring triangle to i is obtuse, this can yield negative values. A mixed scheme is used where a fixed fraction of the triangle

area is used when it has an obtuse angle:

$$A_i^{(t)} = \begin{cases} \left(r_{ji}^2 \cot\theta_k + r_{ki}^2 \cot\theta_j\right)/8 & \text{if triangle } t \text{ is acute} \\ A_t/2 & \text{if } \theta_i \text{ is obtuse} \\ A_t/4 & \text{if any of the other angles is obtuse,} \end{cases} \tag{2.32}$$

where A_t is the area of triangle t, given by $A_t = \frac{1}{2} r_{jk} r_{ki} \sin\theta_k$. An example of the area region used when θ_i obtuse is shown in blue in Fig. 2.5.

Vertex extrinsic curvature

Consider the curvature normal vector, $\boldsymbol{H} = H\hat{\boldsymbol{n}} = \nabla^2 \boldsymbol{r}$, where $\hat{\boldsymbol{n}}$ is the normal vector to the surface and the second expression is the Laplace-Beltrami of the surface parametrization. The mean curvature can then be calculated from the cotangent weights[11] of the discretization of the ∇^2-operator [70]. Given as a sum in neighboring triangles,

$$\boldsymbol{H}_i = \frac{1}{4A_i} \sum_t \left(\cot\theta_k \ \boldsymbol{e}_{ij} + \cot\theta_j \ \boldsymbol{e}_{ik}\right) . \tag{2.33}$$

The mean curvature is given up to a sign as $H_i = s|\boldsymbol{H}_i|$, where the sign s is determined through the pre-defined orientation of the surface. This orientation is imprinted in the fixed orientations of each triangular face, for which vertex triplets $t = \{i, j, k\}$ are ordered such that the edge vectors determine the "outward normal" following the right-hand rule. In other words,

$$s = \text{sign}\left[(\boldsymbol{e}_{ji} \times \boldsymbol{e}_{ki}) \cdot \boldsymbol{H}\right] \tag{2.34}$$

Naturally, it follows that the normal to the surface is $\hat{\boldsymbol{n}}_i = s\boldsymbol{H}_i/|\boldsymbol{H}|$.

Vertex intrinsic curvature

The discrete Gaussian curvature at vertex i is given by

$$K_i = \frac{1}{A_i}\left[2\pi - \sum_t \theta_i^{(t)}\right] , \tag{2.35}$$

where $\theta_i^{(t)}$ is the angle adjacent to vertex i in the triangle t of the neighborhood of i. This expression stems from the Gauss-Bonnet formula, Eq. (2.16) applied to the area patch A_i for which $\chi = 1$, and noting that there is no geodesic curvature on the straight boundaries of the vertex area element [70].

2.3.2 Numerical bending energy

It is straightforward to write an expression of the bending energy of the triangulated surfaces from the discretized equations introduced above to calculate the vertex area, and the mean and Gaussian curvatures. However, we first make a distinction between

[11] Without any concern for obtuse triangles in this case.

bulk and *boundary* vertices of the meshed surface S, since only the former contribute to the bending energy. The bulk vertices v are those with a closed 1-ring neighborhood, i.e. where every neighboring vertex to v is part of exactly two of the adjacent triangular faces to v (for example the blue and gray vertices in Fig. 2.5a). In open topologies, such as the rectangular sheets in Chapter 5, the subset of boundary vertices, $v' \in \partial S$ have no associated mean nor Gaussian curvature (for example, the red vertices).

We consider here the Fischer model in Eq. (2.20), since the terms for the Helfrich energy on spherical topologies are contained in these set of equations. The discrete Fischer integral is given by the sum of the energy of each vertex

$$E_{\text{bend}} = \sum_{v \in S} E^v_{\text{bend}} = \sum_{v \in S} A_v \left[k_H \left(H_v - H_0 \right)^2 + k_\Omega \left(\Omega_v - \Omega_0 \right)^2 \right] , \tag{2.36}$$

with the warp given by $\Omega_v^2 = H_v^2 - K_v$. Because of the numerical inaccuracies of the discretization, the latter expression can result in negative values, in which case we set the warp to zero. The area A_v, the mean curvature H_v and the Gaussian curvature K_v are calculated as described in Section 2.3.1.

2.3.3 Numerical stretching energy

We take two different approaches to determine the stretching energy Eq. (2.31): (i) In Chapters 3 and 4, we use numerical integration of the Poisson equation for the stress Eq. (2.29) on the triangulated surface, from which the stretching energy is then calculated from the stress field at each vertex; (ii) In Chapter 5 we use an alternative discrete expression to the energy integral Eq. (2.31) based on a mesh of Hookean springs (see e.g. Ref. [44]). Here we give a rough outline of the two approaches but more details are found in the corresponding chapters. It is important to note that for either of these two approaches, the triangulated surface is not linked to the underlying molecular structure of the physical system in question.

Discrete Hookean mesh

In the spirit of the stress coming from tangential deformations on the surface, the stretching energy can be approximated from spring-like interactions between the vertices on the triangulated surface. Following linear elasticity, the stretching energy at vertex v is given by a sum in its neighboring vertices $\{w\}$,

$$E_{\text{stretch}} = \frac{1}{2} c_s \sum_v \sum_{w \text{ nn } v} \left(|\boldsymbol{r}_v - \boldsymbol{r}_w| - l_0 \right)^2 , \tag{2.37}$$

where c_s is the energy coupling constant, proportional to the Young's modulus, and the rest length l_0 is a constant parameter. The rest length can set as the averaged edge length $l_0 =< r_{vw} >$ over all edges of the mesh. Using this approach is considerably less computationally expensive which is advantageous for the energy-minimization algorithm used to study of tubulin assemblies of Chapter 5. Furthermore, since we are precisely interested in shape deformations, it is possible to get rid of any pre-stress introduced when using an averaged edge value as a constant rest length.

Numerical integration

Just like we did for the surface curvatures, we can calculate the stress field at each vertex in the meshed surface. In this case, this is done by finding numerical solutions to the Poisson equation for the stress. In particular, consider the dimensionless stress function at vertex v,

$$\nabla_v^2 \hat{\sigma}_v = -\delta K_v \,. \tag{2.38}$$

Using the discrete cotangent formula for the Laplace-Beltrami operator discussed above and in Ref. [70], we can integrate this equation for a given the source term δK_v. The stretching energy trivially follows as

$$E_{\text{stretch}} = \frac{Y}{2} \sum_v A_v \hat{\sigma}_v^2 \,. \tag{2.39}$$

We use this approach for the closed crystalline systems in Chapters 3 and 4, as the physical system has an inaccessibly large number of lattice sites. In this case, the underlying structure is coarse grained as the triangulated mesh, such that each vertex patch corresponds to a large number of lattice sites.

The numerical integration of the stress has the further advantage that we do not need to make any assumptions about the rest length on the mesh, and thus the triangulation can be arbitrarily irregular. This is convenient for systems where we keep the surface shapes fixed, since it prevents introducing any pre-stress when constructing the mesh (see Section B.1 in Chapter 3 for more details).